

# Overturning Pathways Control AMOC Weakening in CMIP6 Models

Baker J.A.<sup>1</sup>, Bell M.J.<sup>1</sup>, Jackson L.C.<sup>1</sup>, Renshaw R.<sup>1</sup>, Vallis G.K.<sup>2</sup>, Watson A.J.<sup>2</sup>, Wood R.A.<sup>1</sup>

<sup>1</sup> Met Office, UK.

<sup>2</sup> University of Exeter, UK.

Corresponding author: Jonathan Baker ([jonathan.baker@metoffice.gov.uk](mailto:jonathan.baker@metoffice.gov.uk))

## Index terms

4532 General circulation (1218, 1222); 4512 Currents; 4513 Decadal ocean variability (1616, 1635, 3305, 4215); 4568 Turbulence, diffusion, and mixing processes (4490)

## Keywords

AMOC, overturning, pathways, weakening, constraint, CMIP6

## Key Points:

- The magnitude of 21<sup>st</sup> century AMOC weakening in CMIP6 models is correlated with an AMOC pathway into the Indo-Pacific Ocean.
- The real-world “Indo-Pacific diffusive” AMOC pathway inferred from observation-based estimates was used to constrain future AMOC weakening.
- Under high-end greenhouse gas forcing, AMOC weakening based on this emergent constraint relationship ranges from 29% to 61% by 2100.

## **Abstract**

Future projections indicate the AMOC will weaken and shoal in response to global warming, but models disagree widely over the amount of weakening. We analyse projected AMOC weakening in 27 CMIP6 climate models, in terms of changes in three return pathways of the AMOC. The branch of the AMOC that returns through diffusive upwelling in the Indo-Pacific, but does not later upwell in the Southern Ocean, is particularly sensitive to warming, in part, because shallowing of the deep flow prevents it from entering the Indo-Pacific via the Southern Ocean. The present-day strength of this Indo-Pacific pathway provides a strong constraint on the projected AMOC weakening. However, estimates of this pathway using four observationally-based methods imply a wide range of AMOC weakening under the SSP5-8.5 scenario of 29% to 61% by 2100. Our results suggest that improved observational constraints on this pathway would substantially reduce uncertainty in 21<sup>st</sup> century AMOC decline.

## **Plain Language Summary**

Changes in the Atlantic Meridional Overturning Circulation (AMOC), an ocean conveyor belt that moves warm water northwards into the North Atlantic Ocean, would have wide-ranging impacts on our climate. The AMOC is predicted to weaken as the climate warms during the 21<sup>st</sup> century, but the extent of weakening differs among climate models. We show that AMOC weakening is greatest in models with a large exchange of water between the AMOC and the Indo-Pacific Ocean along a specific pathway. The magnitude of this ocean pathway, inferred from four observation-based estimates of the global overturning circulation, is uncertain. We use these estimates, and the relationship between the aforementioned ocean pathway and AMOC weakening across many climate models, to predict how the real-world AMOC will change. They indicate that by 2100 the AMOC will weaken by 29% to 61% under a high greenhouse gas emission scenario. This emphasises the importance of constraining the ocean's overturning pathways to reduce uncertainty in future AMOC weakening and to improve climate models so that they represent these pathways more realistically.

## **1. Introduction**

The Atlantic Meridional Overturning Circulation (AMOC) is widely predicted to weaken over the 21<sup>st</sup> century (e.g., Cheng et al., 2013; Weijer et al., 2020), but the magnitude of this change is uncertain in the latest Coupled Model Intercomparison Project (CMIP6). Understanding the mechanisms responsible for the large inter-model spread is crucial to

predict the transient response of the AMOC to increased greenhouse gas concentrations. The ocean's overturning pathways are an important determinant of the equilibrium response of the AMOC to climate forcing (Baker et al., 2020, 2021; Nadeau & Jansen, 2020) and they may therefore also play a role in determining its transient response. We hypothesise that the wide range in the AMOC's transient response to climate forcing among CMIP6 models is due to differences in the historical magnitude of their overturning pathways.

Changes in the Meridional Overturning Circulation (MOC) influence global and regional climate change on seasonal to millennial timescales by changing the ocean's transport of heat, freshwater, and carbon (Buckley & Marshall, 2016; Rahmstorf, 2015; Weijer et al., 2019). How the AMOC changes over the 21<sup>st</sup> century will impact many aspects of the climate (Bellomo et al., 2021; Hu et al., 2020; Liu et al., 2020), so constraining its future response to warming is vital.

The most comprehensive predictions of future changes in climate are provided by CMIP6, a multi-model ensemble of climate simulations (Eyring et al., 2016; O'Neill et al., 2016). In model intercomparison projects, the weakening of the AMOC induced by increasing greenhouse gas (GHG) forcing tends to be greater in models with a stronger control AMOC, so its present-day strength can be used to constrain future weakening (e.g., Cheng et al., 2013; Gregory et al., 2005; Weaver et al., 2012; Weijer et al., 2020; Winton et al., 2014). Several mechanisms have been proposed to explain this dependence. These include the impact of northern sea-ice extent and its subsequent retreat on North Atlantic Ocean heat loss (Levermann et al., 2007), changes in the kinetic energy of the North Atlantic (Gregory & Tailleux, 2011), changes in Labrador Sea convection (Rugenstein et al., 2013), and North Atlantic salinity differences (Jackson et al., 2020). These arguments are based on differences in the mean state and response of the North Atlantic that ultimately affect North Atlantic convection. In contrast, we use the CMIP6 ensemble to investigate the cause of the inter-model spread in AMOC weakening and its dependence on the historical AMOC strength by analysing the model overturning pathways (e.g., Lumpkin & Speer, 2007; Talley, 2013) that return deep waters formed in the North Atlantic to their origin.

The pathways that return NADW to the surface in the present-day ocean either upwell in the Southern Ocean (SO) driven by the SO westerly winds (e.g., Toggweiler & Samuels, 1998) or in the Atlantic and Indo-Pacific Oceans driven by diffusion (e.g., Munk & Wunsch, 1998). Diffusive upwelling in the Indo-Pacific Ocean may significantly affect the equilibrium state of

the global overturning circulation (Ferrari et al., 2017; Jones & Cessi, 2016; Newsom & Thompson, 2018; Thompson et al., 2016); however, its impact on shorter, transient timescales is less clear. Transient changes in the AMOC in response to GHG forcing are believed to be instigated by changes in the North Atlantic buoyancy forcing (Dixon et al., 1999; Stouffer et al., 2006), although the strengthening and poleward shift of the Southern Ocean westerly winds found under high-end warming scenarios in CMIP6 models (Deng et al., 2022) may also impact the AMOC. The equilibrium AMOC probably shoaled in cooler, glacial climates, decoupling the upper and lower cells of the MOC and thus isolating the AMOC from the Indo-Pacific Ocean (Baker et al., 2020, 2021; Ferrari et al., 2014; Nadeau & Jansen, 2020). The AMOC may also shoal in response to GHG forcing with its transient response investigated in idealised models (e.g., Bonan et al., 2022; Chang & Jansen, 2022; Sun et al., 2020). Sun et al. (2020) show that the Indo-Pacific overturning circulation responds rapidly to GHG forcing, weakening to compensate changes in the AMOC through communication between the North Atlantic and Indo-Pacific Oceans via wave processes. By analysing the overturning pathways under varying GHG forcing, we can infer the importance (if any) of Indo-Pacific and Southern Ocean processes on the transient response of the AMOC.

The main questions we seek to answer are:

- What are the historical overturning pathways in the CMIP6 ensemble and how do they change in a warmer climate?
- How does the transient weakening of the AMOC depend on the historical overturning pathways, and what mechanisms are responsible for these dependencies?
- Can we use estimates of the real-world overturning pathways to constrain future AMOC weakening?

## **2. Data and Methods**

### **2.1. CMIP6 Models and observation-based data**

We analyse the overturning pathways in the CMIP6 historical (1850-2014) simulation (Eyring et al., 2016) and in the Scenario Model Intercomparison Project (ScenarioMIP; O'Neill et al., 2016) experiments (2015-2100). The ScenarioMIP experiments represent different Shared Socioeconomic Pathways (SSP's; Riahi et al., 2017) that result in varying radiative forcing and thus warming by 2100. These range from low-end (SSP1-2.6 ("ssp126")) to high-end (SSP5-8.5 ("ssp585")) forcing scenarios. We focus on ssp585 since the AMOC response to forcing is greatest. The monthly-mean overturning mass

streamfunction (Griffies et al., 2016) is produced by 49 models for the historical simulation, 26 models for ssp126 and 27 models for ssp585 (Table S1). We analyse the overturning streamfunction in depth space, and in density space when it is available, using a single ensemble member from each model (Table S1). We average the monthly-mean overturning streamfunction over 1850-2014 in the historical simulation and over 2080-2100 in the ScenarioMIP experiments.

We estimate the real-world overturning pathways from three global ocean reanalyses that assimilate observations into an ocean model: “GloRanV14” (updated version of “GloSea5” e.g., Baker et al., 2022) over 2000-2021, the “Estimating the Circulation and Climate of the Ocean” (ECCOV4; Cessi, 2019; Forget et al., 2015) over 1992-2015 and a robust diagnostic simulation of Lee et al. (2019) that assimilates long-term averaged hydrographic data. We also use the MOC estimate from the inverse model of Lumpkin & Speer (2007) that uses hydrographic data measured over 1987-1996.

## 2.2. Method to separate the overturning pathways

We calculate the time-mean overturning pathways following the method of Baker et al. (2020, 2021) with a few modifications. We define the AMOC herein as the mid-depth cell in the Atlantic basin that is often referred to as the North Atlantic Deep Water (NADW) cell. The maximum strength of the AMOC in the North Atlantic is defined as “AMOC<sub>max</sub>”. We refer to each pathway (Table S3) of the MOC as a pathway of NADW, although the density of this water mass changes as it is transported through the ocean.

To separate the pathways, we use the zonally-averaged meridional overturning streamfunction in the Atlantic and Indo-Pacific basins, and in the Southern Ocean (SO), defined as all latitudes south of 34.5°S, we use the globally-integrated meridional overturning streamfunction (Figure 1). The dynamics of the SO are dominated by the effects of the SO winds, which generate an upper cell and indirectly strengthen a lower eddy-induced cell by tilting the SO isopycnals. We partition the AMOC transport southwards across 34.5°S into that advected into the upper and lower cells of the SO (Figure 1). The transport into the SO lower cell (“NADW\_IP<sub>lower</sub>”) must ultimately upwell in the Indo-Pacific basin, whereas that transported into the upper cell either upwells in the SO and returns to the Atlantic basin (the “Atlantic wind pathway”; “NADW\_At<sub>wind</sub>”) or it is transported by zonal flows into the Indo-Pacific basin (“NADW\_IP<sub>upper</sub>”; not present in Figure 1 but we account for this pathway in our calculations). The total pathway into the Indo-Pacific basin either upwells diffusively in

this basin without later upwelling in the SO (the Indo-Pacific diffusive pathway;  
 “NADW\_IP<sub>diffu</sub>”) or it upwells initially via diffusion and later via the SO upper cell (the Indo-  
 Pacific wind pathway; “NADW\_IP<sub>wind</sub>”). The total SO wind pathway (“NADW\_wind<sub>total</sub>”) is  
 equal to the sum of the Indo-Pacific and Atlantic wind pathways, and it is therefore equal to  
 the total upwelling by the SO upper cell (Figure 1).

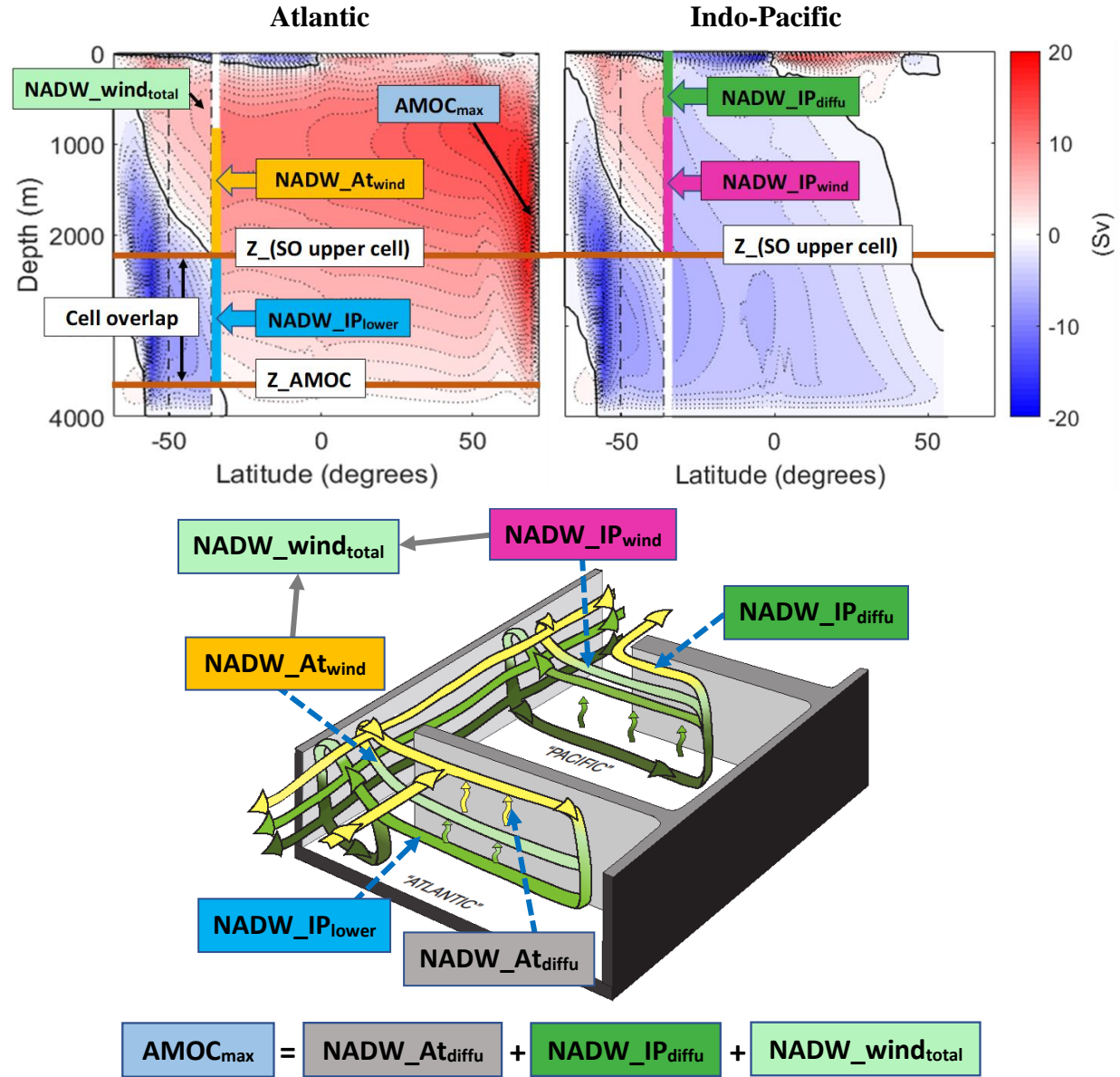


**Figure 1.** (upper) Meridional overturning streamfunction (Sverdrups (Sv); 2 Sv contours) from Baker et al. (2020; 2021), illustrating the method used to separate the overturning pathways. North of 34.5°S (right-hand vertical dashed lines), the streamfunction is plotted for the model Atlantic (left) and Indo-Pacific (right). The global-integrated streamfunction is plotted in the Southern Ocean. The solid black contour is the 0-Sv streamline. Each pathway, except “NADW\_wind<sub>total</sub>”, is equal to the net volume of water flowing from the northern basin into the Southern Ocean over the depth of the associated coloured vertical line at 34.5°S. (lower) Illustration of the overturning pathways.

The Atlantic diffusive pathway (“NADW\_ $A_{diffu}$ ”) upwells NADW in the Atlantic basin before returning northwards, that is, the streamlines of the AMOC are closed within the Atlantic basin. The sum of the three main pathways analysed; the Atlantic diffusive pathway (“NADW\_ $A_{diffu}$ ”), the total SO wind pathway (“NADW\_ $wind_{total}$ ”) and the Indo-Pacific diffusive pathway (“NADW\_ $IP_{diffu}$ ”), are equal to “AMOC $_{max}$ ” (Figure 1 and Table S3). These pathways define the processes by which North Atlantic origin waters are returned to the surface; these waters either upwell in the Atlantic or Indo-Pacific basins via diffusion or they upwell in the SO via the SO winds. Further modifications to the method of Baker et al. (2020, 2021) and the equations used to calculate the pathways (eq. S1-S5) are described in the Supporting Information.

The overturning pathways are more accurately represented in density space since ocean currents tend to flow along isopycnals (Hallberg & Gnanadesikan, 2006). We compare the overturning pathways calculated in depth and density space in five models (Figure S1). Although there are quantitative differences in density space, we expect the qualitative findings of this study to remain valid (see Supporting Information).

### 3. Historical MOC and overturning pathways

#### 3.1. MOC

We first examine the historical (1850-2014) overturning streamfunction and the associated overturning pathways. In all models, the Atlantic has a clockwise, mid-depth cell (i.e., the AMOC), whereas the Indo-Pacific has an expansive anti-clockwise cell. The historical AMOC strength (“AMOC $_{max}$ ”) ranges from ~10 Sv to ~37 Sv, and there is significant inter-model spread in the overturning pathways (Figure 2, S2).

#### 3.2. Absolute overturning pathways

Since the sum of the Atlantic and Indo-Pacific diffusive pathways and the total SO wind pathway are equal to “AMOC $_{max}$ ”, we might expect the historical AMOC strength to correlate with the magnitude of each pathway. While the AMOC strength has a strong, positive correlation with the Atlantic and Indo-Pacific diffusive pathways, it is insignificantly ( $p>0.05$ ) anti-correlated with the total SO wind pathway (Figure 2a-c). This is because there are a cluster of models with weak total SO wind pathways, yet strong AMOC’s (left side of Figure 2b) because they have large Indo-Pacific diffusive pathways (right side of Figure 2c). The remaining models show a positive correlation between the AMOC strength and the total SO wind pathway.

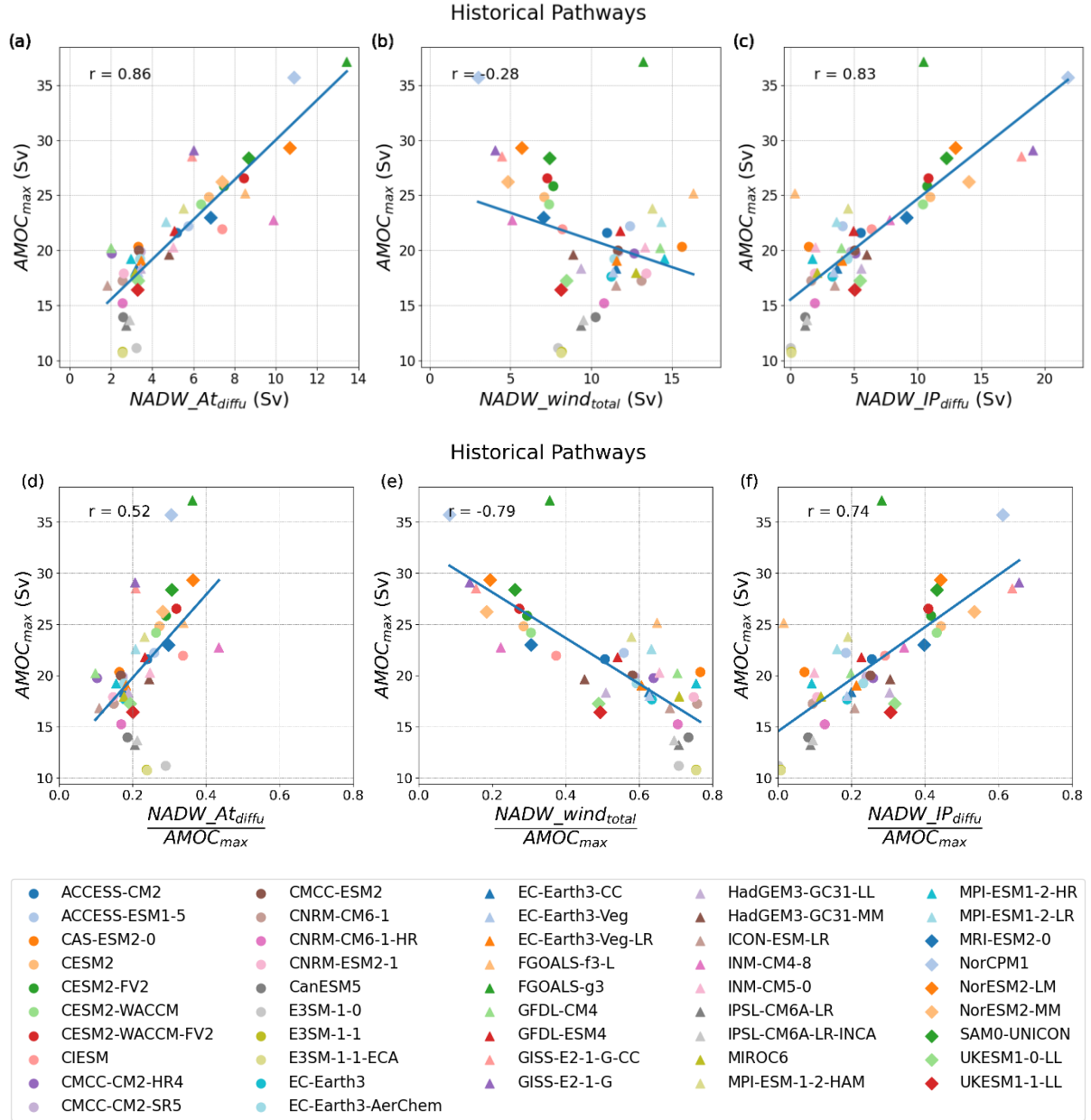


**Figure 2.** (upper) Overturning pathways and (lower) overturning pathways relative to the maximum AMOC strength in the North Atlantic, “AMOC<sub>max</sub>”, calculated in depth space and averaged over the historical simulation (1850-2100), plotted against “AMOC<sub>max</sub>”. The Atlantic diffusive pathway, “NADW\_At<sub>diffu</sub>”, the total SO wind pathway, “NADW\_wind<sub>total</sub>” and the Indo-Pacific diffusive pathway, “NADW\_IP<sub>diffu</sub>” are plotted. The line of best fit and the Pearson correlation coefficient are shown.

### 3.3. Relative overturning pathways

We also find similar relationships, but with lower correlations, between the historical AMOC strength and the overturning pathways relative to this AMOC strength i.e., the relative contribution of each pathway to “AMOC<sub>max</sub>” (Figure 2d-e). However, the “relative” total SO wind pathway is significantly anti-correlated with AMOC strength. Thus, models with lower



“relative” total SO wind pathways tend to have stronger AMOC’s due, in part, to reasons stated in Section 3.2. The “relative” total SO wind and Indo-Pacific diffusive pathways have similar ranges but opposing relationships with “AMOC<sub>max</sub>” (Figure 2d,e). The ensemble-mean “relative” total SO wind pathway (55%) is greater than the ensemble-mean “relative” Indo-Pacific (22%) and Atlantic (23%) diffusive pathways (Figure 2d-f).

#### 4. Transient response of AMOC and overturning pathways to warming

##### 4.1. AMOC weakening

All warming scenarios in the CMIP6 ensemble predict a weakening of the AMOC over the 21<sup>st</sup> century, but there is a large inter-model variation. The AMOC weakens by 9%–42% (mean value of 24%) in ssp126 (Figure 3a) and by 21%–67% (mean value of 44%) in ssp585 by 2080-2100 (Figure 3d), relative to the historical (1850-2014) mean AMOC for each model. We also find that models with a stronger historical AMOC tend to have greater AMOC weakening (Figure 3a-d), in agreement with previous inter-model comparison studies (e.g., Weaver et al., 2012; Weijer et al., 2020; Winton et al., 2014). The strength of this relationship increases at higher rates of warming i.e., from ssp126 to ssp585. In addition to the AMOC weakening, the Indo-Pacific MOC also weakens (Figure S3), compensating changes in the AMOC (in agreement with Sun et al. (2020)).

##### 4.2. Changes in the overturning pathways

We analyse the association between the magnitude of the historical overturning pathways and AMOC weakening in ssp585 (Figure 3e-g). Both the Atlantic and Indo-Pacific diffusive pathways are positively correlated with AMOC weakening (i.e., these pathways tend to be larger in models with greater weakening). In contrast, the total SO wind pathway is anti-correlated with AMOC weakening. The Indo-Pacific diffusive pathway explains 81% of the variance in AMOC weakening (i.e.,  $r=0.90$  in ssp585; Figure 3g), notably higher than the 55% of the variance explained by the historical AMOC strength (i.e.,  $r=0.74$  in ssp585; Figure 3d). The AMOC weakening has a lower dependence on the Atlantic diffusive and total SO wind pathways ( $r=0.61$  and  $r=-0.62$  respectively), which therefore reduce the dependence of AMOC weakening on the historical AMOC strength. Thus, the primary reason for the

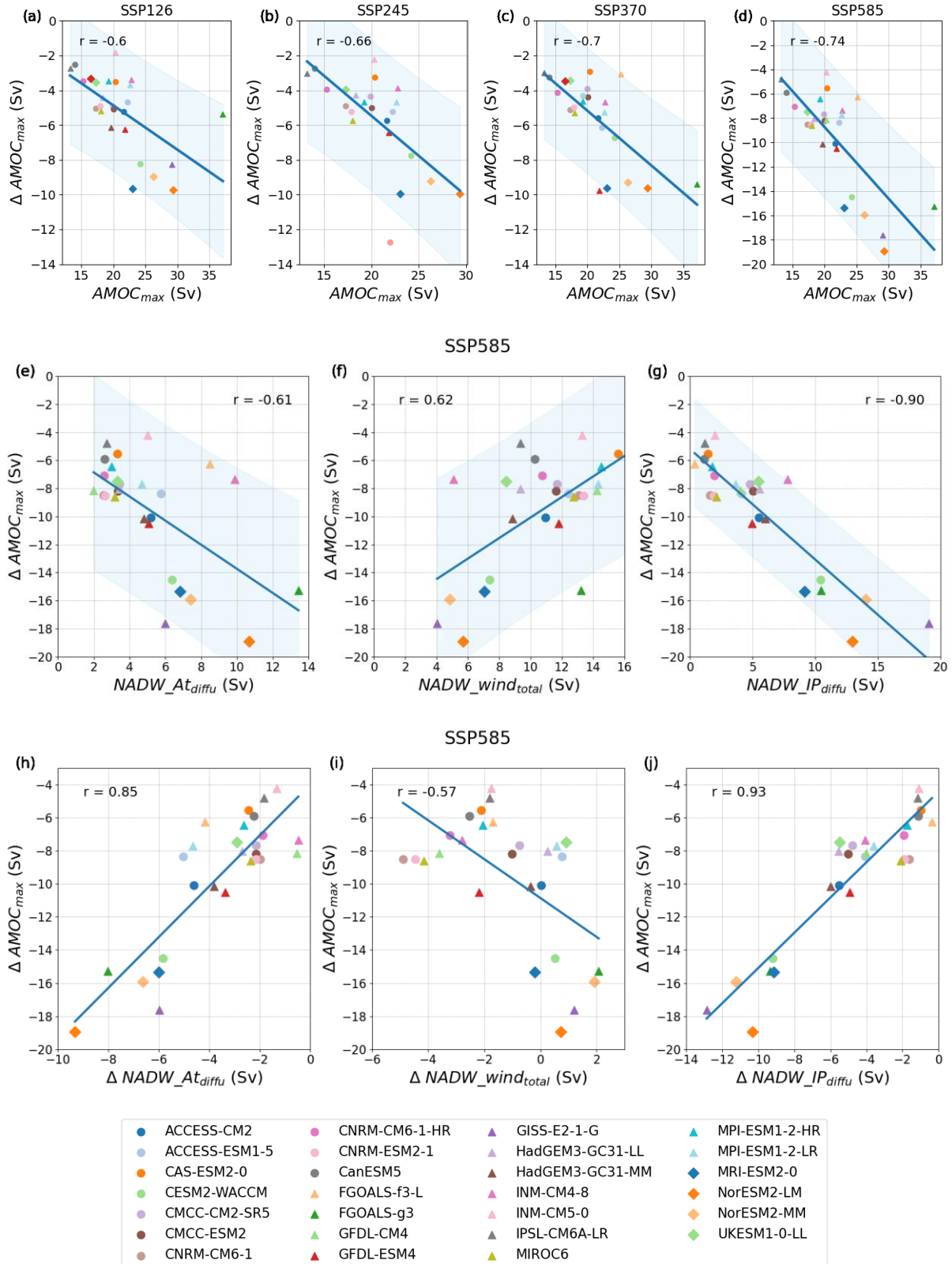


**Figure 3.** (upper panels) The historical average AMOC strength, “AMOC<sub>max</sub>”, plotted against the change in “AMOC<sub>max</sub>” by 2080-2100 in (i) ssp126 (ii) ssp245 (iii) ssp370 and (iv) ssp585. (center panels) Historical overturning pathways and (lower panels) their change, plotted against the change in “AMOC<sub>max</sub>” by 2080-2100 in ssp585. Blue shading represents the 95% prediction interval. Further details are specified in Figure 2.

strong dependence of AMOC weakening on the historical AMOC strength is its strong dependence on the Indo-Pacific diffusive pathway. The aforementioned correlation coefficients are lower for ssp126 than ssp585, but the AMOC weakening still has a higher correlation with the Indo-Pacific diffusive pathway ( $r=0.78$ , not shown) than with the historical AMOC strength ( $r=0.6$ ; Figure 3a).

We now look at how the overturning pathways in ssp585 change over the 21<sup>st</sup> century (Figure 4) to understand why the AMOC weakening is strongly dependent on the Indo-Pacific diffusive pathway (and less dependent on the other pathways). Although the AMOC weakens in all models, the rate and magnitude of weakening vary greatly (Figure 4a,e). By 2100, all models predict a decrease in the Indo-Pacific and Atlantic diffusive pathways, but the total SO wind pathway has a mixed response (Figure 4b-d,f-h). This pathway typically contributes little to the change in AMOC strength (Figure 4c,g) so has little impact on the relationship between the Indo-Pacific diffusive pathway and AMOC weakening. This is probably because changes in the SO winds are too small to weaken the SO upper cell and because the SO overturning is slow to respond to changes in the AMOC (Chang & Jansen, 2022; Sun et al., 2020). By 2100, the decrease in the Indo-Pacific diffusive pathway has a large inter-model spread ( $\sim 1$  Sv to  $\sim 13$  Sv), whereas the Atlantic diffusive pathway tends to have a smaller decrease (Figure 4). Changes in these pathways are highly correlated ( $r=0.76$ , not shown).

The weakening of the AMOC is strongly correlated with decreases in the Atlantic and Indo-Pacific diffusive pathways (Figure 3h,j). In contrast, changes in the total SO wind pathway are weakly anti-correlated with AMOC weakening due to the subset of models with a strong Indo-Pacific diffusive pathway weakening most despite little change in their total SO wind pathways (Figure 3i). We also find changes in the Indo-Pacific diffusive pathway are almost inversely proportional to its historical magnitude ( $r=-0.97$ ; not shown), whereas changes in the Atlantic and total SO wind pathways are less dependent on their historical magnitudes ( $r=-0.7$  and  $r=-0.45$  respectively).

#### 4.3. Mechanisms

The almost proportional relationship between the historical Indo-Pacific diffusive pathway and its decrease by 2080-2100 is due, in part, to this pathway weakening to zero in many models during the 21<sup>st</sup> century (Figure 4d). The historical magnitude of this pathway therefore sets an upper limit on its weakening and constrains the AMOC's decline. Thus, while reduced North Atlantic convection probably causes the AMOC weakening, the

magnitude of decline is modulated by the magnitude of the Indo-Pacific diffusive pathway, with changes communicated rapidly via wave processes (Sun et al., 2020). This pathway decreases, in part, because the “cell overlap” between the AMOC and the SO lower cell decreases in response to GHG forcing, reducing the main pathway for NADW to enter the Indo-Pacific Ocean (Figure S3; see Baker et al., 2020, 2021; Nadeau & Jansen, 2020).

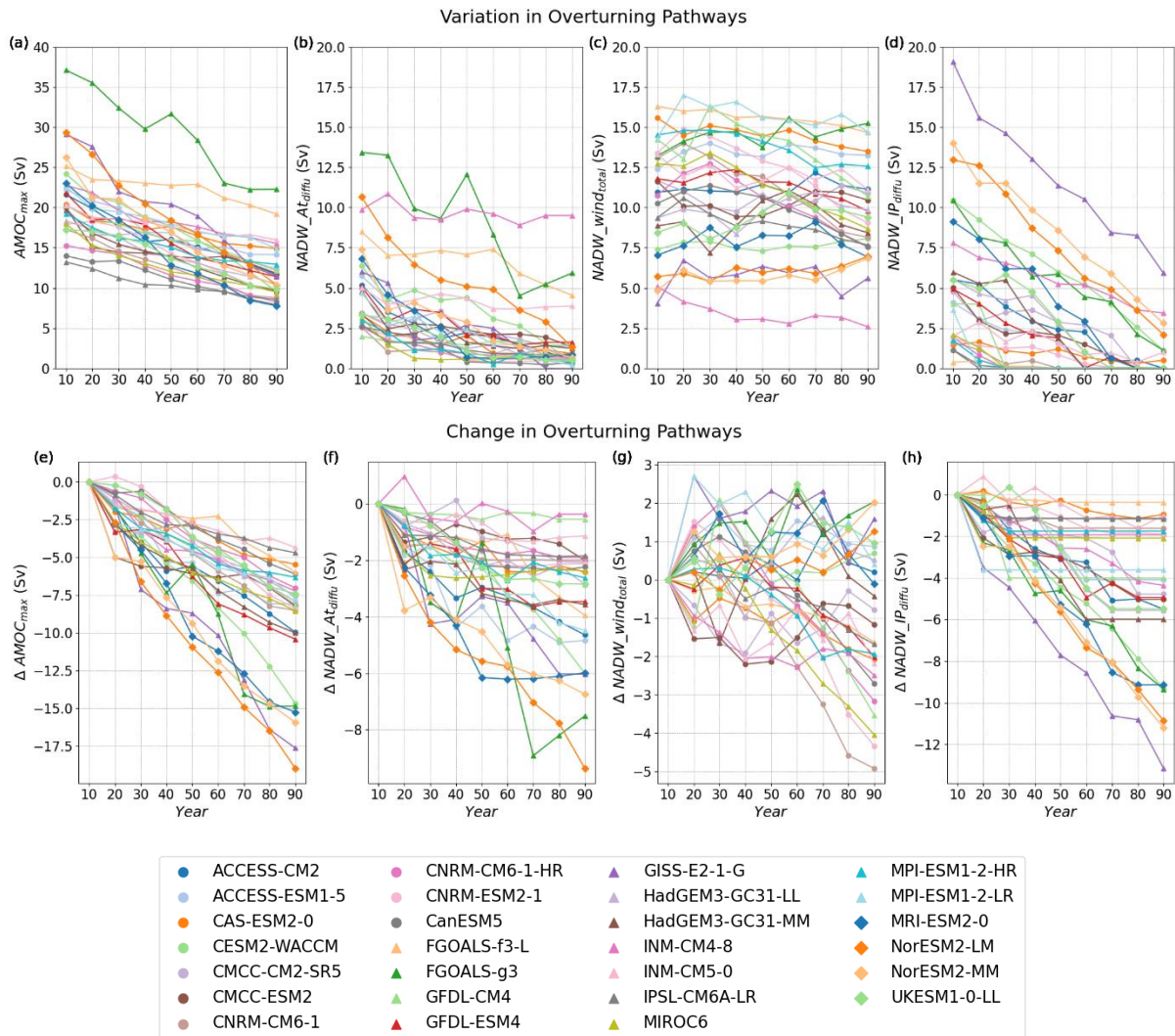


**Figure 4.** Timeseries of the AMOC strength and overturning pathways showing (upper panels) their absolute magnitudes, and (lower panels) the change in their magnitudes from the historical average (1850-2014). The historical average is labelled as 2010 (“10”) with average values in “ssp585” calculated in 10-year intervals from 2015-2095 (labelled “20” to “90”).

## 5. Constraining future AMOC weakening

Since the weakening of the AMOC is strongly related to the magnitude of the historical Indo-Pacific diffusive pathway, we use this emergent constraint relationship to predict future weakening of the real-world AMOC. Using the AMOC strength and overturning pathways inferred from observation-based MOC estimates (Table S2), the emergent constraint

relationship (Figure 3f) predicts large differences in AMOC decline by 2080-2100 under ssp585 forcing; 29% (range of 8%–50% from the 95% prediction interval in Figure 3f) from ECCOv4, 35% (14%–56%) from an inverse model estimate (Lumpkin & Speer, 2007), 41% (26%–56%) from a robust diagnostic simulation (Lee et al., 2019) and 61% (41%–81%) from GloRanV14 (Table S2). Under ssp126 forcing, the emergent constraint predicts a weaker AMOC decline for each observation-based estimate, ranging from 17% to 32% (Table S2).

Although the prediction intervals of the emergent constraint relationship are large (Figure 3f), they are significantly smaller than the equivalent analysis using the historical AMOC strength to constrain the weakening (Figure 3d). Each of the observation-based estimates of AMOC strength (except the robust diagnostic simulation) and a direct observational estimate at 26.5°N of 16.9 Sv (Moat et al., 2022) imply a weakening under ssp585 forcing of ~41% (6%–76%) by 2100. Despite high confidence in the AMOC strength observed at 26.5°N, AMOC weakening constrained by this estimate is highly uncertain. Thus, even though the magnitude of the Indo-Pacific diffusive pathway is uncertain, AMOC weakening based on this pathway has a comparable uncertainty (8%–81%) to that based on the AMOC strength. Between observation-based estimates, their South Atlantic transports are similar, but their total SO wind pathways and thus Indo-Pacific diffusive pathways differ (Table S2). Reducing uncertainty in the strength of the SO upper cell at 34.5°S and thus in these pathways would increase confidence in estimates of future AMOC decline.

## **6. Discussion and Conclusions**

The response of the AMOC to GHG forcing in the CMIP6 multi-model ensemble is uncertain. Under low-end forcing (SSP1-2.6), by 2080-2100 the AMOC in each model weakens on average by 24% (range of 9%–42% across the ensemble) relative to its historical mean AMOC, while under high-end forcing (SSP5-8.5), the average weakening increases to 44% (range of 21%–67%). We show that the partition of the historical (1850-2014) overturning pathways largely determines how the AMOC responds to future climate forcing. Specifically, the historical pathway of North Atlantic origin waters that upwells diffusively in the Indo-Pacific Ocean but is not later upwelled in the Southern Ocean (SO) is strongly related to the weakening of the AMOC. Under high-end forcing, this historical Indo-Pacific diffusive pathway explains 81% of the variance in the AMOC weakening across the ensemble compared to only 55% that is explained by the historical AMOC strength. This emergent constraint relationship on AMOC weakening can be used to predict future changes

in the AMOC. Due to large uncertainty in observation-based estimates of the real-world Indo-Pacific diffusive pathway, they imply a wide range of AMOC weakening by 2080-2100 of 17%–32% (best estimates) under SSP1-2.6 forcing and of 29%–61% under SSP5-8.5 forcing.

Mechanisms proposed to explain the association between the weakening of the AMOC and its historical strength (e.g., Cheng et al., 2013; Weaver et al., 2012; Weijer et al., 2020) largely focus on the mean state of the North Atlantic (e.g., Jackson et al., 2020; Levermann et al., 2007). We argue that because AMOC weakening has a stronger dependence on the Indo-Pacific diffusive pathway than the historical AMOC strength, these North Atlantic based mechanisms may not fully explain this relationship. Although changes in North Atlantic convection likely cause the AMOC to shoal and weaken, the magnitude of this weakening is largely controlled by the magnitude of the Indo-Pacific diffusive pathway.

As the AMOC shoals, the “cell overlap” between the AMOC and the SO lower cell decreases, reducing the pathway into the Indo-Pacific Ocean (e.g., Baker et al., 2020, 2021; Nadeau & Jansen, 2020). The weakening of the AMOC is strongly dependent on the historical magnitude of the Indo-Pacific diffusive pathway, in part, because its magnitude acts as an upper limit on its decrease. Changes in the pathway that upwells in the Atlantic are also strongly related to changes in the Indo-Pacific diffusive pathway, whereas the pathway that upwells North Atlantic origin waters via the SO upper cell has only a weak response.

The structure and strength of the AMOC is thought to be set by the buoyancy forcing, the vertical diffusivity, the SO wind stress and mesoscale eddies, among other factors (Bellomo et al., 2021). The historical overturning pathways are therefore dependent on these model processes and forcings. Thus, accurately representing these processes in models is crucial to obtain a historical MOC and AMOC response that is realistic. Improved observational estimates of the real-world overturning pathways would reduce uncertainty in our prediction of AMOC weakening. They may also suggest how climate models can improve their representation of the historical MOC and thus changes in the AMOC, which could also improve their oceanic transports of heat, salinity and carbon (e.g., Aldama-Campino et al., 2020; Heuzé, 2021; Sun et al., 2022). Future research could attempt to understand the cause of the large inter-model spread in the historical overturning pathways and AMOC strength.

## **Acknowledgements**

JAB, LCJ and RAW were supported by the European Union’s Horizon 2020 research and innovation programme (grant no. 820970, TiPES project). LCJ, MJB and RAW were supported by the Met Office Hadley Centre Climate Programme funded by BEIS.

## Open Research

The CMIP6 data used in this study is available from ESGF (<https://esgf-index1.ceda.ac.uk/search/cmip6-ceda/>) with references listed in Table S1. MOC estimates from ECCOV4, a robust diagnostic simulation and an inverse model were taken from Cessi (2019), Lee et al., 2019 and Lumpkin & Speer (2007) respectively. MOC estimates from GloRanV14 (funded by the E.U. Copernicus Marine Service) are available through Zenodo: <https://doi.org/10.5281/zenodo.7649266> (Baker and Renshaw, 2023).

## References

- Aldama-Campino, A., Fransner, F., Ödalen, M., Groeskamp, S., Yool, A., Döös, K., & Nycander, J. (2020). Meridional Ocean Carbon Transport. *Global Biogeochemical Cycles*, 34(9), e2019GB006336. <https://doi.org/10.1029/2019GB006336>
- Baker, J. A., Watson, A. J., & Vallis, G. K. (2020). Meridional overturning circulation in a multibasin model. Part i: Dependence on southern ocean buoyancy forcing. *Journal of Physical Oceanography*, 50(5), 1159–1178. <https://doi.org/10.1175/JPO-D-19-0135.1>
- Baker, J. A., Watson, A. J., & Vallis, G. K. (2021). Meridional Overturning Circulation in a Multibasin Model. Part II: Sensitivity to Diffusivity and Wind in Warm and Cool Climates. *Journal of Physical Oceanography*, 51(6), 1813–1828. <https://doi.org/10.1175/JPO-D-20-0121.1>
- Bellomo, K., Angeloni, M., Corti, S., & von Hardenberg, J. (2021). Future climate change shaped by inter-model differences in Atlantic meridional overturning circulation response. *Nature Communications* 2021 12:1, 12(1), 1–10. <https://doi.org/10.1038/s41467-021-24015-w>
- Bonan, D. B., Thompson, A. F., Newsom, E. R., Sun, S., & Rugenstein, M. (2022). Transient and Equilibrium Responses of the Atlantic Overturning Circulation to Warming in Coupled Climate Models: The Role of Temperature and Salinity. *Journal of Climate*, 35(15), 5173–5193. <https://doi.org/10.1175/jcli-d-21-0912.1>
- Buckley, M. W., & Marshall, J. (2016). Observations, inferences, and mechanisms of the Atlantic Meridional Overturning Circulation: A review. *Reviews of Geophysics*, 54(1), 5–63. <https://doi.org/10.1002/2015RG000493>
- Cessi, P. (2019). The Global Overturning Circulation. <https://doi.org/10.1146/annurev-marine-010318-095241>, 11, 249–270. <https://doi.org/10.1146/annurev-marine-010318-095241>
- Chang, C.-Y., & Jansen, M. F. (2022). The time-dependent response of a two-basin ocean to a sudden surface temperature change. *Journal of Climate*, 1–34. <https://doi.org/10.1175/jcli-d-21-0821.1>

- 417 Cheng, W., Chiang, J. C. H., & Zhang, D. (2013). Atlantic Meridional Overturning Circulation (AMOC)  
418 in CMIP5 Models: RCP and Historical Simulations. *Journal of Climate*, 26(18), 7187–7197.  
419 <https://doi.org/10.1175/JCLI-D-12-00496.1>
- 420 Deng, K., Azorin-Molina, C., Yang, S., Hu, C., Zhang, G., Minola, L., & Chen, D. (2022). Changes of  
421 Southern Hemisphere westerlies in the future warming climate. *Atmospheric Research*, 270,  
422 106040. <https://doi.org/10.1016/J.ATMOSRES.2022.106040>
- 423 Dixon, K. W., Delworth, T. L., Spelman, M. J., & Stouffer, R. J. (1999). The influence of transient  
424 surface fluxes on North Atlantic overturning in a coupled GCM Climate Change Experiment.  
425 *Geophysical Research Letters*, 26(17), 2749–2752. <https://doi.org/10.1029/1999GL900571>
- 426 Eyring, V., Bony, S., Meehl, G. A., Senior, C. A., Stevens, B., Stouffer, R. J., & Taylor, K. E. (1937).  
427 Overview of the Coupled Model Intercomparison Project Phase 6 (CMIP6) experimental design  
428 and organization. *Geosci. Model Dev*, 9. <https://doi.org/10.5194/gmd-9-1937-2016>
- 429 Ferrari, R., Jansen, M. F., Adkins, J. F., Burke, A., Stewart, A. L., & Thompson, A. F. (2014). Antarctic  
430 sea ice control on ocean circulation in present and glacial climates. *Proceedings of the National*  
431 *Academy of Sciences of the United States of America*, 111(24), 8753–8758.  
432 [https://doi.org/10.1073/PNAS.1323922111/SUPPL\\_FILE/PNAS.201323922SI.PDF](https://doi.org/10.1073/PNAS.1323922111/SUPPL_FILE/PNAS.201323922SI.PDF)
- 433 Ferrari, R., Nadeau L-P, Marshall, D., Allison, L. C., & Johnson, H. L. (2017). A Model of the Ocean  
434 Overturning Circulation with Two Closed Basins and a Reentrant Channel. *J. Phys. Oceanogr.*,  
435 47, 2887–2906. <https://doi.org/10.1175/JPO-D-16-0223.1>
- 436 Forget, G., Campin, J. M., Heimbach, P., Hill, C. N., Ponte, R. M., & Wunsch, C. (2015). ECCO version  
437 4: An integrated framework for non-linear inverse modeling and global ocean state estimation.  
438 *Geoscientific Model Development*, 8(10), 3071–3104. [https://doi.org/10.5194/GMD-8-3071-](https://doi.org/10.5194/GMD-8-3071-2015)  
439 2015
- 440 Gregory, J. M., Dixon, K. W., Stouffer, R. J., Weaver, A. J., Driesschaert, E., Eby, M., Fichet, T.,  
441 Hasumi, H., Hu, A., Jungclaus, J. H., Kamenkovich, I. v., Levermann, A., Montoya, M., Murakami,  
442 S., Nawrath, S., Oka, A., Sokolov, A. P., & Thorpe, R. B. (2005). *A model intercomparison of*  
443 *changes in the Atlantic thermohaline circulation in response to increasing atmospheric*  
444 *CO<sub>2</sub> concentration*. <https://doi.org/10.1029/2005GL023209>
- 445 Gregory, J. M., & Tailleux, R. (2011). Kinetic energy analysis of the response of the Atlantic  
446 meridional overturning circulation to CO<sub>2</sub>-forced climate change. *Climate Dynamics*, 37(5),  
447 893–914. <https://doi.org/10.1007/S00382-010-0847-6/FIGURES/11>
- 448 Griffies, S. M., Danabasoglu, G., Durack, P. J., Adcroft, A. J., Balaji, V., Böning, C. W., Chassignet, E. P.,  
449 Curchitser, E., Deshayes, J., Drange, H., Fox-Kemper, B., Gleckler, P. J., Gregory, J. M., Haak, H.,  
450 Hallberg, R. W., Heimbach, P., Hewitt, H. T., Holland, D. M., Ilyina, T., ... Yeager, S. G. (2016).  
451 OMIP contribution to CMIP6: Experimental and diagnostic protocol for the physical component  
452 of the Ocean Model Intercomparison Project. *Geoscientific Model Development*, 9(9), 3231–  
453 3296. <https://doi.org/10.5194/GMD-9-3231-2016>
- 454 Hallberg, R., & Gnanadesikan, A. (2006). The Role of Eddies in Determining the Structure and  
455 Response of the Wind-Driven Southern Hemisphere Overturning: Results from the Modeling  
456 Eddies in the Southern Ocean (MESO) Project. *Journal of Physical Oceanography*, 36(12), 2232–  
457 2252. <https://doi.org/10.1175/JPO2980.1>



- 458 Heuzé, C. (2021). Antarctic Bottom Water and North Atlantic Deep Water in CMIP6 models. *Ocean*  
459 *Science*, 17(1), 59–90. <https://doi.org/10.5194/os-17-59-2021>
- 460 Hu, A., van Roekel, L., Weijer, W., Garuba, O. A., Cheng, W., & Nadiga, B. T. (2020). Role of AMOC in  
461 Transient Climate Response to Greenhouse Gas Forcing in Two Coupled Models. *Journal of*  
462 *Climate*, 33(14), 5845–5859. <https://doi.org/10.1175/JCLI-D-19-1027.1>
- 463 Jackson, L. C., Roberts, M. J., Hewitt, H. T., Iovino, D., Koenigk, T., Meccia, V. L., Roberts, C. D.,  
464 Ruprich-Robert, Y., & Wood, R. A. (2020). Impact of ocean resolution and mean state on the  
465 rate of AMOC weakening. *Climate Dynamics*, 55(7–8), 1711–1732.  
466 <https://doi.org/10.1007/s00382-020-05345-9>
- 467 Jones, C. S., & Cessi, P. (2016). Interbasin Transport of the Meridional Overturning Circulation.  
468 *Journal of Physical Oceanography*, 46(4), 1157–1169. <https://doi.org/10.1175/JPO-D-15-0197.1>
- 469 Lee, S. K., Lumpkin, R., Baringer, M. O., Meinen, C. S., Goes, M., Dong, S., Lopez, H., & Yeager, S. G.  
470 (2019). Global Meridional Overturning Circulation Inferred From a Data-Constrained Ocean &  
471 Sea-Ice Model. *Geophysical Research Letters*, 46(3), 1521–1530.  
472 <https://doi.org/10.1029/2018GL080940>
- 473 Levermann, A., Mignot, J., Nawrath, S., & Rahmstorf, S. (2007). *The Role of Northern Sea Ice Cover*  
474 *for the Weakening of the Thermohaline Circulation under Global Warming*.  
475 <https://doi.org/10.1175/JCLI4232.1>
- 476 Liu, W., Fedorov, A. v., Xie, S. P., & Hu, S. (2020). Climate impacts of a weakened Atlantic meridional  
477 overturning circulation in a warming climate. *Science Advances*, 6(26).  
478 [https://doi.org/10.1126/SCIADV.AAZ4876/SUPPL\\_FILE/AAZ4876\\_SM.PDF](https://doi.org/10.1126/SCIADV.AAZ4876/SUPPL_FILE/AAZ4876_SM.PDF)
- 479 Lumpkin, R., & Speer, K. (2007). Global Ocean Meridional Overturning. *Journal of Physical*  
480 *Oceanography*, 37(10), 2550–2562. <https://doi.org/10.1175/JPO3130.1>
- 481 Menary, M. B., Hodson, D. L. R., Robson, J. I., Sutton, R. T., Wood, R. A., & Hunt, J. A. (2015).  
482 Exploring the impact of CMIP5 model biases on the simulation of North Atlantic decadal  
483 variability. *Geophysical Research Letters*, 42(14), 5926–5934.  
484 <https://doi.org/10.1002/2015GL064360>
- 485 Munk, W., & Wunsch, C. (1998). Abyssal recipes II: energetics of tidal and wind mixing. *Deep Sea*  
486 *Research Part I: Oceanographic Research Papers*, 45(12), 1977–2010.  
487 [https://doi.org/10.1016/S0967-0637\(98\)00070-3](https://doi.org/10.1016/S0967-0637(98)00070-3)
- 488 Nadeau, L. P., & Jansen, M. F. (2020). Overturning Circulation Pathways in a Two-Basin Ocean Model.  
489 *Journal of Physical Oceanography*, 50(8), 2105–2122. <https://doi.org/10.1175/JPO-D-20-0034.1>
- 490 Newsom, E. R., & Thompson, A. F. (2018). Reassessing the Role of the Indo-Pacific in the Ocean’s  
491 Global Overturning Circulation. *Geophysical Research Letters*, 45(22), 12,422–12,431.  
492 <https://doi.org/10.1029/2018GL080350>
- 493 O’Neill, B. C., Tebaldi, C., van Vuuren, D. P., Eyring, V., Friedlingstein, P., Hurtt, G., Knutti, R., Kriegler,  
494 E., Lamarque, J.-F., Lowe, J., Meehl, G. A., Moss, R., Riahi, K., & Sanderson, B. M. (2016). The  
495 Scenario Model Intercomparison Project (ScenarioMIP) for CMIP6. *Geosci. Model Dev*, 9, 3461–  
496 3482. <https://doi.org/10.5194/gmd-9-3461-2016>

- 497 Rahmstorf, S. (2015). Exceptional twentieth-century slowdown in Atlantic Ocean overturning  
498 circulation. *Nat. Clim. Chang.*, 5(5), 475–480. <https://doi.org/10.1038/nclimate2554>
- 499 Riahi, K., van Vuuren, D. P., Kriegler, E., Edmonds, J., O'Neill, B. C., Fujimori, S., Bauer, N., Calvin, K.,  
500 Dellink, R., Fricko, O., Lutz, W., Popp, A., Cuaresma, J. C., KC, S., Leimbach, M., Jiang, L., Kram,  
501 T., Rao, S., Emmerling, J., ... Tavoni, M. (2017). The Shared Socioeconomic Pathways and their  
502 energy, land use, and greenhouse gas emissions implications: An overview. *Global*  
503 *Environmental Change*, 42, 153–168. <https://doi.org/10.1016/J.GLOENVCHA.2016.05.009>
- 504 Rugenstein, M. A. A., Winton, M., Stouffer, R. J., Griffies, S. M., & Hallberg, R. (2013). Northern High-  
505 Latitude Heat Budget Decomposition and Transient Warming. *Journal of Climate*, 26(2), 609–  
506 621. <https://doi.org/10.1175/JCLI-D-11-00695.1>
- 507 Schmittner, A., Latif, M., & Schneider, B. (2005). Model projections of the North Atlantic  
508 thermohaline circulation for the 21st century assessed by observations. *Geophysical Research*  
509 *Letters*, 32(23), 1–4. <https://doi.org/10.1029/2005GL024368>
- 510 Stouffer, R. J., Yin, J., Gregory, J. M., Dixon, K. W., Spelman, M. J., Hurlin, W., Weaver, A. J., Eby, M.,  
511 Flato, G. M., Hasumi, H., Hu, A., Jungclaus, J. H., Kamenkovich, I. v., Levermann, A., Montoya,  
512 M., Murakami, S., Nawrath, S., Oka, A., Peltier, W. R., ... Weber, S. L. (2006). Investigating the  
513 Causes of the Response of the Thermohaline Circulation to Past and Future Climate Changes.  
514 *Journal of Climate*, 19(8), 1365–1387. <https://doi.org/10.1175/JCLI3689.1>
- 515 Sun, S., Thompson, A. F., & Eisenman, I. (2020). Transient Overturning Compensation between  
516 Atlantic and Indo-Pacific Basins. *Journal of Physical Oceanography*, 50(8), 2151–2172.  
517 <https://doi.org/10.1175/JPO-D-20-0060.1>
- 518 Sun, S., Thompson, A. F., Xie, S. P., & Long, S. M. (2022). Indo-Pacific Warming Induced by a  
519 Weakening of the Atlantic Meridional Overturning Circulation. *Journal of Climate*, 35(2), 815–  
520 832. <https://doi.org/10.1175/JCLI-D-21-0346.1>
- 521 Talley, L. D. (2013). Closure of the global overturning circulation through the Indian, Pacific, and  
522 southern oceans. *Oceanography*, 26(1), 80–97. <https://doi.org/10.5670/OCEANOLOG.2013.07>
- 523 Thompson, A. F., Stewart, A. L., & Bischoff, T. (2016). A Multibasin Residual-Mean Model for the  
524 Global Overturning Circulation. *Journal of Physical Oceanography*, 46(9), 2583–2604.  
525 <https://doi.org/10.1175/JPO-D-15-0204.1>
- 526 Toggweiler, J. R., & Samuels, B. (1998). On the Ocean's Large-Scale Circulation near the Limit of No  
527 Vertical Mixing. *Journal of Physical Oceanography*, 28(9), 1832–1852.  
528 [https://doi.org/10.1175/1520-0485\(1998\)028](https://doi.org/10.1175/1520-0485(1998)028)
- 529 Weaver, A. J., Sedláček, J., Eby, M., Alexander, K., Cresspin, E., Fichet, T., Philippon-Berthier, G.,  
530 Joos, F., Kawamiy, M., Matsumoto, K., Steinacher, M., Tachiiri, K., Tokos, K., Yoshimori, M., &  
531 Zickfeld, K. (2012). Stability of the Atlantic meridional overturning circulation: A model  
532 intercomparison. *Geophysical Research Letters*, 39(20), 20709.  
533 <https://doi.org/10.1029/2012GL053763>
- 534 Weijer, W., Cheng, W., Drijfhout, S. S., Fedorov, A. v., Hu, A., Jackson, L. C., Liu, W., McDonagh, E. L.,  
535 Mecking, J. v., & Zhang, J. (2019). Stability of the Atlantic Meridional Overturning Circulation: A  
536 Review and Synthesis. *Journal of Geophysical Research: Oceans*, 124(8), 5336–5375.  
537 <https://doi.org/10.1029/2019JC015083>

- 538 Weijer, W., Cheng, W., Garuba, O. A., Hu, A., & Nadiga, B. T. (2020). CMIP6 Models Predict  
539 Significant 21st Century Decline of the Atlantic Meridional Overturning Circulation. *Geophysical*  
540 *Research Letters*, 47(12), e2019GL086075. <https://doi.org/10.1029/2019GL086075>
- 541 Winton, M., Anderson, W. G., Delworth, T. L., Griffies, S. M., Hurlin, W. J., & Rosati, A. (2014). Has  
542 coarse ocean resolution biased simulations of transient climate sensitivity? *Geophysical*  
543 *Research Letters*, 41(23), 8522–8529. <https://doi.org/10.1002/2014GL061523>
- 544
- 545 Baker, J. A., Renshaw, R., Jackson, L. C., Dubois, C., Iovino, D., Zuo, H., Perez, R. C., Dong, S., Kersalé,  
546 M., Mayer, M., Mayer, J., Speich, S., and Lamont, T. (2022): Overturning and heat transport  
547 variations in the South Atlantic in an ocean reanalysis ensemble, State Planet Discuss. [preprint],  
548 <https://doi.org/10.5194/sp-2022-8>, in review.
- 549 Baker J., & Renshaw R. (2023). GloRanV14 ocean reanalysis MOC data [Data set].  
550 Zenodo. <https://doi.org/10.5281/zenodo.7649266>
- 551 Moat, B. I., Frajka-Williams, E., Smeed, D. A., Rayner, D., Johns, W. E., Baringer, M. O., et al. (2022).  
552 Atlantic meridional overturning circulation observed by the RAPID-MOCHA-WBTS (RAPID-Meridional  
553 Overturning Circulation and Heatflux Array-Western Boundary Time Series) array at 26N from 2004  
554 to 2020 (v2020.2). [Dataset]. British Oceanographic Data Centre, Natural Environment Research  
555 Council. <https://doi.org/10.5285/e91b10af-6f0a-7fa7-e053-6c86abc05a09>
- 556 **References From the Supporting Information**
- 557 Aldama-Campino, A., Fransner, F., Ödalen, M., Groeskamp, S., Yool, A., Döös, K., & Nycander, J.  
558 (2020). Meridional Ocean Carbon Transport. *Global Biogeochemical Cycles*, 34(9),  
559 e2019GB006336. <https://doi.org/10.1029/2019GB006336>
- 560 Baker, J. A., Watson, A. J., & Vallis, G. K. (2020). Meridional overturning circulation in a multibasin  
561 model. Part i: Dependence on southern ocean buoyancy forcing. *Journal of Physical*  
562 *Oceanography*, 50(5), 1159–1178. <https://doi.org/10.1175/JPO-D-19-0135.1>
- 563 Baker, J. A., Watson, A. J., & Vallis, G. K. (2021). Meridional Overturning Circulation in a Multibasin  
564 Model. Part II: Sensitivity to Diffusivity and Wind in Warm and Cool Climates. *Journal of*  
565 *Physical Oceanography*, 51(6), 1813–1828. <https://doi.org/10.1175/JPO-D-20-0121.1>
- 566 Bellomo, K., Angeloni, M., Corti, S., & von Hardenberg, J. (2021). Future climate change shaped by  
567 inter-model differences in Atlantic meridional overturning circulation response. *Nature*  
568 *Communications* 2021 12:1, 12(1), 1–10. <https://doi.org/10.1038/s41467-021-24015-w>
- 569 Bonan, D. B., Thompson, A. F., Newsom, E. R., Sun, S., & Rugenstein, M. (2022). Transient and  
570 Equilibrium Responses of the Atlantic Overturning Circulation to Warming in Coupled Climate  
571 Models: The Role of Temperature and Salinity. *Journal of Climate*, 35(15), 5173–5193.  
572 <https://doi.org/10.1175/jcli-d-21-0912.1>
- 573 Buckley, M. W., & Marshall, J. (2016). Observations, inferences, and mechanisms of the Atlantic  
574 Meridional Overturning Circulation: A review. *Reviews of Geophysics*, 54(1), 5–63.  
575 <https://doi.org/10.1002/2015RG000493>
- 576 Cessi, P. (2019). The Global Overturning Circulation. <https://doi.org/10.1146/annurev-marine-010318-095241>, 11, 249–270. <https://doi.org/10.1146/annurev-marine-010318-095241>
- 577

- 578 Chang, C.-Y., & Jansen, M. F. (2022). The time-dependent response of a two-basin ocean to a sudden  
579 surface temperature change. *Journal of Climate*, 1–34. <https://doi.org/10.1175/jcli-d-21-0821.1>
- 580 Cheng, W., Chiang, J. C. H., & Zhang, D. (2013). Atlantic Meridional Overturning Circulation (AMOC)  
581 in CMIP5 Models: RCP and Historical Simulations. *Journal of Climate*, 26(18), 7187–7197.  
582 <https://doi.org/10.1175/JCLI-D-12-00496.1>
- 583 Deng, K., Azorin-Molina, C., Yang, S., Hu, C., Zhang, G., Minola, L., & Chen, D. (2022). Changes of  
584 Southern Hemisphere westerlies in the future warming climate. *Atmospheric Research*, 270,  
585 106040. <https://doi.org/10.1016/J.ATMOSRES.2022.106040>
- 586 Dixon, K. W., Delworth, T. L., Spelman, M. J., & Stouffer, R. J. (1999). The influence of transient  
587 surface fluxes on North Atlantic overturning in a coupled GCM Climate Change Experiment.  
588 *Geophysical Research Letters*, 26(17), 2749–2752. <https://doi.org/10.1029/1999GL900571>
- 589 Eyring, V., Bony, S., Meehl, G. A., Senior, C. A., Stevens, B., Stouffer, R. J., & Taylor, K. E. (1937).  
590 Overview of the Coupled Model Intercomparison Project Phase 6 (CMIP6) experimental design  
591 and organization. *Geosci. Model Dev*, 9. <https://doi.org/10.5194/gmd-9-1937-2016>
- 592 Ferrari, R., Jansen, M. F., Adkins, J. F., Burke, A., Stewart, A. L., & Thompson, A. F. (2014). Antarctic  
593 sea ice control on ocean circulation in present and glacial climates. *Proceedings of the National*  
594 *Academy of Sciences of the United States of America*, 111(24), 8753–8758.  
595 [https://doi.org/10.1073/PNAS.1323922111/SUPPL\\_FILE/PNAS.201323922SI.PDF](https://doi.org/10.1073/PNAS.1323922111/SUPPL_FILE/PNAS.201323922SI.PDF)
- 596 Ferrari, R., Nadeau L-P, Marshall, D., Allison, L. C., & Johnson, H. L. (2017). A Model of the Ocean  
597 Overturning Circulation with Two Closed Basins and a Reentrant Channel. *J. Phys. Oceanogr.*,  
598 47, 2887–2906. <https://doi.org/10.1175/JPO-D-16-0223.1>
- 599 Forget, G., Campin, J. M., Heimbach, P., Hill, C. N., Ponte, R. M., & Wunsch, C. (2015). ECCO version  
600 4: An integrated framework for non-linear inverse modeling and global ocean state estimation.  
601 *Geoscientific Model Development*, 8(10), 3071–3104. [https://doi.org/10.5194/GMD-8-3071-](https://doi.org/10.5194/GMD-8-3071-2015)  
602 2015
- 603 Gregory, J. M., Dixon, K. W., Stouffer, R. J., Weaver, A. J., Driesschaert, E., Eby, M., Fichefet, T.,  
604 Hasumi, H., Hu, A., Jungclaus, J. H., Kamenkovich, I. v, Levermann, A., Montoya, M., Murakami,  
605 S., Nawrath, S., Oka, A., Sokolov, A. P., & Thorpe, R. B. (2005). *A model intercomparison of*  
606 *changes in the Atlantic thermohaline circulation in response to increasing atmospheric*  
607 *CO<sub>2</sub> concentration*. <https://doi.org/10.1029/2005GL023209>
- 608 Gregory, J. M., & Tailleux, R. (2011). Kinetic energy analysis of the response of the Atlantic  
609 meridional overturning circulation to CO<sub>2</sub>-forced climate change. *Climate Dynamics*, 37(5),  
610 893–914. <https://doi.org/10.1007/S00382-010-0847-6/FIGURES/11>
- 611 Griffies, S. M., Danabasoglu, G., Durack, P. J., Adcroft, A. J., Balaji, V., Böning, C. W., Chassignet, E. P.,  
612 Curchitser, E., Deshayes, J., Drange, H., Fox-Kemper, B., Gleckler, P. J., Gregory, J. M., Haak, H.,  
613 Hallberg, R. W., Heimbach, P., Hewitt, H. T., Holland, D. M., Ilyina, T., ... Yeager, S. G. (2016).  
614 OMIP contribution to CMIP6: Experimental and diagnostic protocol for the physical component  
615 of the Ocean Model Intercomparison Project. *Geoscientific Model Development*, 9(9), 3231–  
616 3296. <https://doi.org/10.5194/GMD-9-3231-2016>
- 617 Hallberg, R., & Gnanadesikan, A. (2006). The Role of Eddies in Determining the Structure and  
618 Response of the Wind-Driven Southern Hemisphere Overturning: Results from the Modeling

- 619 Eddies in the Southern Ocean (MESO) Project. *Journal of Physical Oceanography*, 36(12), 2232–  
620 2252. <https://doi.org/10.1175/JPO2980.1>
- 621 Heuzé, C. (2021). Antarctic Bottom Water and North Atlantic Deep Water in CMIP6 models. *Ocean*  
622 *Science*, 17(1), 59–90. <https://doi.org/10.5194/os-17-59-2021>
- 623 Hu, A., van Roekel, L., Weijer, W., Garuba, O. A., Cheng, W., & Nadiga, B. T. (2020). Role of AMOC in  
624 Transient Climate Response to Greenhouse Gas Forcing in Two Coupled Models. *Journal of*  
625 *Climate*, 33(14), 5845–5859. <https://doi.org/10.1175/JCLI-D-19-1027.1>
- 626 Jackson, L. C., Roberts, M. J., Hewitt, H. T., Iovino, D., Koenigk, T., Meccia, V. L., Roberts, C. D.,  
627 Ruprich-Robert, Y., & Wood, R. A. (2020). Impact of ocean resolution and mean state on the  
628 rate of AMOC weakening. *Climate Dynamics*, 55(7–8), 1711–1732.  
629 <https://doi.org/10.1007/s00382-020-05345-9>
- 630 Jones, C. S., & Cessi, P. (2016). Interbasin Transport of the Meridional Overturning Circulation.  
631 *Journal of Physical Oceanography*, 46(4), 1157–1169. <https://doi.org/10.1175/JPO-D-15-0197.1>
- 632 Lee, S. K., Lumpkin, R., Baringer, M. O., Meinen, C. S., Goes, M., Dong, S., Lopez, H., & Yeager, S. G.  
633 (2019). Global Meridional Overturning Circulation Inferred From a Data-Constrained Ocean &  
634 Sea-Ice Model. *Geophysical Research Letters*, 46(3), 1521–1530.  
635 <https://doi.org/10.1029/2018GL080940>
- 636 Levermann, A., Mignot, J., Nawrath, S., & Rahmstorf, S. (2007). *The Role of Northern Sea Ice Cover*  
637 *for the Weakening of the Thermohaline Circulation under Global Warming*.  
638 <https://doi.org/10.1175/JCLI4232.1>
- 639 Liu, W., Fedorov, A. v., Xie, S. P., & Hu, S. (2020). Climate impacts of a weakened Atlantic meridional  
640 overturning circulation in a warming climate. *Science Advances*, 6(26).  
641 [https://doi.org/10.1126/SCIADV.AAZ4876/SUPPL\\_FILE/AAZ4876\\_SM.PDF](https://doi.org/10.1126/SCIADV.AAZ4876/SUPPL_FILE/AAZ4876_SM.PDF)
- 642 Lumpkin, R., & Speer, K. (2007). Global Ocean Meridional Overturning. *Journal of Physical*  
643 *Oceanography*, 37(10), 2550–2562. <https://doi.org/10.1175/JPO3130.1>
- 644 Menary, M. B., Hodson, D. L. R., Robson, J. I., Sutton, R. T., Wood, R. A., & Hunt, J. A. (2015).  
645 Exploring the impact of CMIP5 model biases on the simulation of North Atlantic decadal  
646 variability. *Geophysical Research Letters*, 42(14), 5926–5934.  
647 <https://doi.org/10.1002/2015GL064360>
- 648 Munk, W., & Wunsch, C. (1998). Abyssal recipes II: energetics of tidal and wind mixing. *Deep Sea*  
649 *Research Part I: Oceanographic Research Papers*, 45(12), 1977–2010.  
650 [https://doi.org/10.1016/S0967-0637\(98\)00070-3](https://doi.org/10.1016/S0967-0637(98)00070-3)
- 651 Nadeau, L. P., & Jansen, M. F. (2020). Overturning Circulation Pathways in a Two-Basin Ocean Model.  
652 *Journal of Physical Oceanography*, 50(8), 2105–2122. <https://doi.org/10.1175/JPO-D-20-0034.1>
- 653 Newsom, E. R., & Thompson, A. F. (2018). Reassessing the Role of the Indo-Pacific in the Ocean’s  
654 Global Overturning Circulation. *Geophysical Research Letters*, 45(22), 12,422–12,431.  
655 <https://doi.org/10.1029/2018GL080350>
- 656 O’Neill, B. C., Tebaldi, C., van Vuuren, D. P., Eyring, V., Friedlingstein, P., Hurtt, G., Knutti, R., Kriegler,  
657 E., Lamarque, J.-F., Lowe, J., Meehl, G. A., Moss, R., Riahi, K., & Sanderson, B. M. (2016). The

- 658 Scenario Model Intercomparison Project (ScenarioMIP) for CMIP6. *Geosci. Model Dev*, 9, 3461–  
659 3482. <https://doi.org/10.5194/gmd-9-3461-2016>
- 660 Rahmstorf, S. (2015). Exceptional twentieth-century slowdown in Atlantic Ocean overturning  
661 circulation. *Nat. Clim. Chang.*, 5(5), 475–480. <https://doi.org/10.1038/nclimate2554>
- 662 Riahi, K., van Vuuren, D. P., Kriegler, E., Edmonds, J., O'Neill, B. C., Fujimori, S., Bauer, N., Calvin, K.,  
663 Dellink, R., Fricko, O., Lutz, W., Popp, A., Cuaresma, J. C., KC, S., Leimbach, M., Jiang, L., Kram,  
664 T., Rao, S., Emmerling, J., ... Tavoni, M. (2017). The Shared Socioeconomic Pathways and their  
665 energy, land use, and greenhouse gas emissions implications: An overview. *Global*  
666 *Environmental Change*, 42, 153–168. <https://doi.org/10.1016/J.GLOENVCHA.2016.05.009>
- 667 Rugenstein, M. A. A., Winton, M., Stouffer, R. J., Griffies, S. M., & Hallberg, R. (2013). Northern High-  
668 Latitude Heat Budget Decomposition and Transient Warming. *Journal of Climate*, 26(2), 609–  
669 621. <https://doi.org/10.1175/JCLI-D-11-00695.1>
- 670 Schmittner, A., Latif, M., & Schneider, B. (2005). Model projections of the North Atlantic  
671 thermohaline circulation for the 21st century assessed by observations. *Geophysical Research*  
672 *Letters*, 32(23), 1–4. <https://doi.org/10.1029/2005GL024368>
- 673 Stouffer, R. J., Yin, J., Gregory, J. M., Dixon, K. W., Spelman, M. J., Hurlin, W., Weaver, A. J., Eby, M.,  
674 Flato, G. M., Hasumi, H., Hu, A., Jungclaus, J. H., Kamenkovich, I. v., Levermann, A., Montoya,  
675 M., Murakami, S., Nawrath, S., Oka, A., Peltier, W. R., ... Weber, S. L. (2006). Investigating the  
676 Causes of the Response of the Thermohaline Circulation to Past and Future Climate Changes.  
677 *Journal of Climate*, 19(8), 1365–1387. <https://doi.org/10.1175/JCLI3689.1>
- 678 Sun, S., Thompson, A. F., & Eisenman, I. (2020). Transient Overturning Compensation between  
679 Atlantic and Indo-Pacific Basins. *Journal of Physical Oceanography*, 50(8), 2151–2172.  
680 <https://doi.org/10.1175/JPO-D-20-0060.1>
- 681 Sun, S., Thompson, A. F., Xie, S. P., & Long, S. M. (2022). Indo-Pacific Warming Induced by a  
682 Weakening of the Atlantic Meridional Overturning Circulation. *Journal of Climate*, 35(2), 815–  
683 832. <https://doi.org/10.1175/JCLI-D-21-0346.1>
- 684 Talley, L. D. (2013). Closure of the global overturning circulation through the Indian, Pacific, and  
685 southern oceans. *Oceanography*, 26(1), 80–97. <https://doi.org/10.5670/OCEANOLOG.2013.07>
- 686 Thompson, A. F., Stewart, A. L., & Bischoff, T. (2016). A Multibasin Residual-Mean Model for the  
687 Global Overturning Circulation. *Journal of Physical Oceanography*, 46(9), 2583–2604.  
688 <https://doi.org/10.1175/JPO-D-15-0204.1>
- 689 Toggweiler, J. R., & Samuels, B. (1998). On the Ocean's Large-Scale Circulation near the Limit of No  
690 Vertical Mixing. *Journal of Physical Oceanography*, 28(9), 1832–1852.  
691 [https://doi.org/10.1175/1520-0485\(1998\)028](https://doi.org/10.1175/1520-0485(1998)028)
- 692 Weaver, A. J., Sedláček, J., Eby, M., Alexander, K., Cresspin, E., Fichet, T., Philippon-Berthier, G.,  
693 Joos, F., Kawamiy, M., Matsumoto, K., Steinacher, M., Tachiiri, K., Tokos, K., Yoshimori, M., &  
694 Zickfeld, K. (2012). Stability of the Atlantic meridional overturning circulation: A model  
695 intercomparison. *Geophysical Research Letters*, 39(20), 20709.  
696 <https://doi.org/10.1029/2012GL053763>
- 697 Weijer, W., Cheng, W., Drijfhout, S. S., Fedorov, A. v., Hu, A., Jackson, L. C., Liu, W., McDonagh, E. L.,  
698 Mecking, J. v., & Zhang, J. (2019). Stability of the Atlantic Meridional Overturning Circulation: A

- 699        Review and Synthesis. *Journal of Geophysical Research: Oceans*, 124(8), 5336–5375.  
700        <https://doi.org/10.1029/2019JC015083>
- 701        Weijer, W., Cheng, W., Garuba, O. A., Hu, A., & Nadiga, B. T. (2020). CMIP6 Models Predict  
702        Significant 21st Century Decline of the Atlantic Meridional Overturning Circulation. *Geophysical*  
703        *Research Letters*, 47(12), e2019GL086075. <https://doi.org/10.1029/2019GL086075>
- 704        Winton, M., Anderson, W. G., Delworth, T. L., Griffies, S. M., Hurlin, W. J., & Rosati, A. (2014). Has  
705        coarse ocean resolution biased simulations of transient climate sensitivity? *Geophysical*  
706        *Research Letters*, 41(23), 8522–8529. <https://doi.org/10.1002/2014GL061523>
- 707